Proceedings of the IASS 2024 Symposium
Redefining the Art of Structural Design
August 26-30, 2024, Zurich, Switzerland
Philippe Block, Giulia Boller, Catherine DeWolf,
Jacqueline Pauli, Walter Kaufmann (eds.)

Interactive Design of C-shells Using Reduced Parametric Families

Quentin BECKER*, Seiichi SUZUKI, Mark PAULY

* École Polytechnique Fédérale de Lausanne
1015 Lausanne, Switzerland
quentin.becker@epfl.ch

Abstract

Elastic gridshells are a class of planar-to-3D linkages typically composed of straight flexible beams connected via rigid rotational joints. The integration of planar curved flexible beams into these linkages significantly broadens their design space, allowing for a diverse range of deployable configurations. We termed these special types of linkages *C-shells*. The main characteristic of these structures is that they intrinsically encode their deployed states in the shapes of their beams while maintaining a planar and zero-energy assembly state. However, designing a C-shell is not a trivial task due to the freeform shape of their beams and the complex physical behavior emerging from their elastic deformation. To address this challenge, we introduce a computational approach for interactive design exploration of C-shells. We show how we can leverage geometric principles on the arrangement of the beams to efficiently create linkage assemblies that deploy into low-energy states of varied geometries and aesthetics. Our reduced parameterization relies on planar conformal maps that preserve the deployability of a reference linkage while generating a spectrum of smooth design variations. To explore design alternatives, users can interactively modify the beam connectivity, starting from a selection of predefined parametric grid topology families. Our interactive tool includes a physics simulation, offering both visual and quantitative feedback on the deployment of the explored designs. We showcase the utility and adaptability of our approach through design studies of a variety of C-shell families.

Keywords: deployable gridshells, design exploration, computational design, physics-based simulation.

1. Introduction

Elastic gridshells are a prominent application of the principle of active bending and are characterized by thin, flexible beams interconnected at scissor joints to form a grid-like structure. This arrangement facilitates intricate deformation behaviors, with beams undergoing large elastic deformation at small strains while rotating around their joints.

Historically, gridshells have utilized straight beams arranged in uniform grids that are deformed to curved 3D geometries by imposing suitable boundary constraints. Recent advancements depart from this shaping principle and instead, arrange the beams in non-uniform configurations. These arrangements introduce kinematic incompatibilities, forcing the structures to buckle out of plane when deployed. Here, a significant advantage lies in the capability to encode target shapes directly into the material system by fine-tuning the distances at which beams connect. However, due to such irregularities, the main disadvantage is their tendency to adopt non-planar states at rest.

In this context, C-shells emerge as a novel class of non-uniform elastic gridshells characterized by the use of curved planar beams with arbitrary cross-sections. Offering a broader design space for constructing free-form surface geometries, C-shells guarantee a planar and stress-free assembly state due to the introduction of rest curvature in the planar beams. In this paper, we introduce an approach for the design

Copyright ©2024 by the authors.
Published in the Proceedings of the IASS Annual Symposium 2024 with permission.

exploration of these structures using a low-dimensional representation of the beam layout. Our reduced parameterization relies on planar conformal maps, preserving the deployability of a reference linkage while generating a spectrum of smooth design variations. We showcase the utility and adaptability of our approach through various C-shell families.

2. Related Work

Smooth Chebyshev nets are the fundamental principle for designing regular elastic gridshells. The most common geometric technique used in architecture to address the design of these gridshells is the so-called compass method, initially proposed by Burkhart and colleagues [1]. Alternative approaches have been proposed based on the duality of isoradial meshes and Chebyshev nets [2], the combination of basic buildings blocks [3] and multi-patch approaches based on optimization methods to approximate intricate geometries [4, 5]. Special attention demands the concept of C-meshes proposed by Liu et al. [6]. C-meshes are classes of deployable grid-shell structures with beams placed orthogonally to a target surface. One particular feature is the existence of C-meshes shaped from straight strips for Chebyshev nets approximating surfaces of constant Gaussian curvature and circular strips for quad grids approximating surfaces with the linear-Weingarten property.

Relevant to our work is the research on non-regular elastic grid-shell structures. X-shells [7] employ straight beams arranged in irregular grids, enabling assembly in a near-planar configuration before deployment into a 3D shape. This method offers designers the ability to iteratively adjust the planar grid layout based on interactive feedback regarding the resulting 3D geometry. Subsequently, optimization is applied to minimize elastic energy in both the flat assembly and deployed states. Recent research on elastic geodesic grids has similarly focused on exploring irregular grid configurations [8, 9, 10]. These studies take advantage of the inherent property of thin lamellas, which are constrained to conform to geodesic curves on a surface owing to their highly anisotropic bending stiffness. Schling and colleagues [11] investigated a distinct type of non-regular grid-shell structure employing asymptotic grids to approximate surfaces with non-positive Gaussian curvature.

The utilization of curved planar ribbons is another aspect relevant to our work. Ren et al. [12] introduced a method that extends weaving techniques to incorporate curved ribbons, offering greater flexibility in the topology of the weaving pattern and resulting in a smoother appearance of the final woven structure. Baek and coworkers [13] explored the impact of in-plane curvatures of ribbons to develop smooth spherical, ellipsoidal, and toroidal triaxial woven structures using a unit-cell approach. Mhatre et al. [14] proposed a deployable circular structure made from elastic beams with constant in-plane curvature. In contrast to our approach, these methods do not explicitly couple beams along their span with rotational joints.

3. Background

We briefly describe the way C-shells are defined, simulated, and deployed as initially proposed in [15]. More details on these aspects can be found in the original paper.

C-shells Parameterization. C-shells are instantiated by manipulating a set of control points in the plane that are interpolated using cubic splines [16], each representing a curved elastic rod. These control points can be further categorized into joints, which are shared among splines, and intermediated control points, which are specific to each spline. We gather both in a single array $\mathbf{q} \in \mathbb{R}^{n_q}$ that defines the degrees of freedom of the system. This parameterization decouples the topology of C-shells from the geometric information encoded in the beam shapes.

Physical Model. Each beam is split into segments at the joints, which are then simulated using the elastic rod model from Bergou and colleagues [17, 18]. At each end of each segment, a rotational joint connects beams belonging to different families by enforcing positional and rotational constraints except for a rotation about the joint normals. Elastic rods are defined by a rest quantities array $\mathbf{p}(\mathbf{q}) \in \mathbb{R}^{n_p}$ (rest lengths and rest geodesic curvatures) extracted from the splines directly so that any layout is at rest and flat when drawn by the designer. The segments are further decomposed into edges, whose positions and orientations are stored in the array $\mathbf{x} \in \mathbb{R}^{n_x}$. Special treatment is given to edges connected at joints, as described in Panetta et al. [7]. Deformations of the linkage are quantified using the elastic energy $E(\mathbf{x}, \mathbf{p})$ that accounts for stretching, bending, and twisting of the linkage beams.

C-shells Deployment. Deployment is achieved by imposing uniform torque at the joints and solving for the equilibrium state $\mathbf{x}^*_{3\mathrm{D}}$ of the whole linkage. Equivalently, we can constrain the average opening angle $\bar{\alpha}(\mathbf{x})$ to a user-defined value [15]. The deployment process is formulated as the following optimization problem

$$\begin{aligned} \mathbf{x}^*_{3\mathrm{D}}(\mathbf{p}, \bar{\alpha}^{\mathrm{tgt}}) := \underset{\mathbf{x}}{\operatorname{argmin}}\, & E(\mathbf{x}, \mathbf{p}) \\ \text{s.t.} \quad & \bar{\alpha}(\mathbf{x}) = \bar{\alpha}^{\mathrm{tgt}}, \end{aligned} \tag{1}$$

where $\bar{\alpha}^{\mathrm{tgt}}$ is the target average opening angle. We additionally pin the three translational and three rotational degrees of freedom of an arbitrary node to eliminate global rigid transformations.

4. Geometry for C-shells

Due to the complex interplay of beam connections and the freeform geometry of beam shapes, the physical deployment of C-shells offers rich geometric behavior that can be difficult to predict by the designer. To aid interactive design, we have found that certain geometric principles based on joint angles and inter-joint distances allow us to qualify the structure's deployability and the sensitivity of its deployed state to the input parameters.

Opening Angles Distributions. The deployment of a C-shell defined in Equation (1) is determined by its average opening angle. Therefore, the distribution of joint angles in the planar rest state naturally impacts the deployability of the structure.

First, the range of this distribution determines whether the C-shell can be deployed by increasing or decreasing joint angles. The difference between the maximum value in the range and π indicates the extent to which the angles can be opened for deployment. Similarly, the difference between the minimum value in the range and 0 represents the degree to which the angles can be closed for deployment.

Second, the extent of the range of the distribution gives an indication of the incompatibility of a C-shell. A narrow angle spectrum indicates a compatible linkage (which stays in plane when deployed) or a conformal variation of one such linkage. On the other hand, a wider opening angle spectrum indicates an incompatible linkage in the vast majority of the cases. For instance, a Klann-like linkage [19] exhibits varying opening angles while remaining compatible. However, any random perturbations to the initial design will likely compromise this property. In practice, they represent a negligible fraction of the designs, which makes the distribution width a valid measure of incompatibility in a linkage.

Inter-Joint Distances. C-shells are parameterized using splines that interpolate joint positions. While intermediate control points are introduced to enrich the space of beam designs, we show in Figure 1 that the deployed shape is less sensitive to their positioning. This observation suggests that, to a first approximation, the overall form of a C-shell is predominantly determined by the arrangement of joints in the plane, rather than the specific placement of intermediate control points.

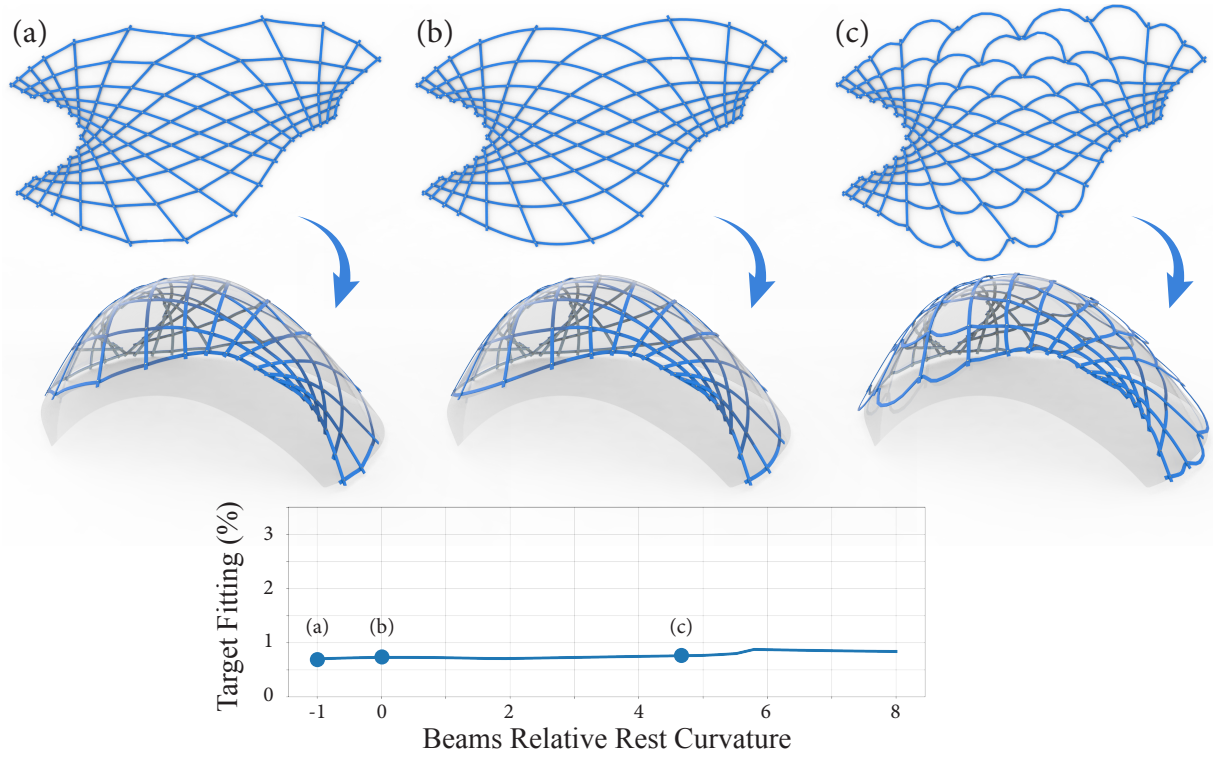


Figure 1: The curvature of segments at rest does not significantly impact the deployed shape if the joint's positions are identical. Designs (a) to (c) share the same joints with varying intermediate control points. The closest deployed state along the deployment path (second row) remains close to the target surface. We report the target deviation as a percentage of the bounding box diagonal of the target surface as a function of the rest curvature relative perturbation.

5. Parametric Families of Deformations

Based on the foundational concepts of C-shells parameterization and deployment, we introduce a practical approach for exploratory design processes. Our method involves a series of interactive editing operations that enable the smooth deformation of an initial 2D linkage design. These 2D deformation maps can be combined arbitrarily to generate design variations. Our physics-based linkage simulation then allows evaluation of the design modifications on the deployed 3D structure.

5.1. Conformal Deformations

Conformal maps preserve the angle distribution and distort the inter-joint distances of an input C-shell layout. In light of the considerations above, they hence allow controlling the deployed shape while preserving the deployability of the initial design.

Planar conformal maps offer a rich space of 2D deformations. The Riemann mapping theorem states that given two simply connected subsets of $\mathbb{R}^2$, there exists a bijective conformal map between them [22]. Such a mapping is unique up to rotations and translations. To control such a conformal map, the user can manipulate the non-self-intersecting closed boundary curve of the linkage. We can then infer the corresponding conformal map using the Boundary First Flattening (BFF) algorithm [21] applied to planar domains. This method solves for a discrete approximation of a conformal map that we apply to our linkage structure to obtain the new beam geometries and joint locations.

Alternatively, we can replace the conformal map with a harmonic parameterization [20]. While harmonic

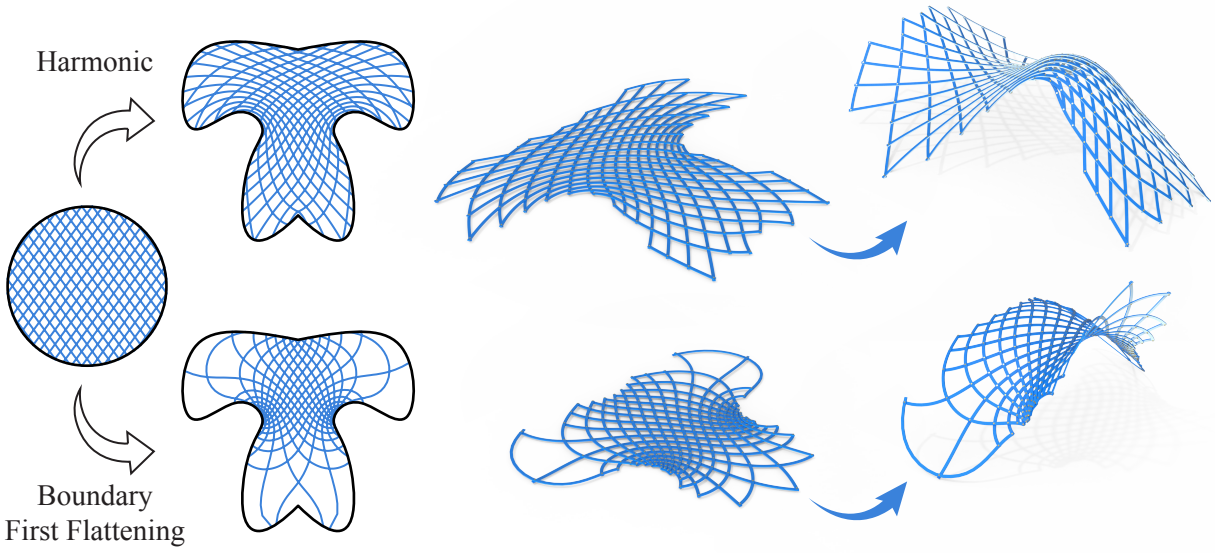


Figure 2: Our tool allows the user to manipulate the domain boundary and deform an initial grid layout according to two strategies. Harmonic parameterization [20] is near-conformal while Boundary First Flattening [21] deforms the input conformally. Larger quadrilaterals are filtered out depending on a user-defined tolerance on their areas. The resulting models can be deployed for further inspection.

maps do not preserve angles, they can reduce area distortion, which leads to a more uniform spacing of joints. Both methods are shown in Figure 2, where we illustrate how a simple regular grid on a unit disk can be transformed to create interesting design variations.

Möbius transforms. As an alternative to editing the linkage boundary, we offer a more direct way to define a specific subset of conformal maps, called *Möbius transforms*. These maps can be created as a composition of three basic transforms: an inverse stereographic projection onto a sphere, a rotation of the sphere about its center, and a projection back to the plane. We expose three parameters to the user: the height of the sphere center and the rotations about the initial plane axes. The first parameter controls the scale of the initial linkage, while the last two parameters allow bringing various kinds of incompatibilities into the linkage. We conceal the x and y coordinates of the sphere center and the rotation about the normal to the design plane since they only rigidly deform the initial layout. Figure 3 illustrates how this simple interface enables effective exploration of design alternatives.

5.2. Attractive and Repulsive Points

Conformal deformations primarily manipulate the geometric properties at a global level, while preserving the deployability of the grid layout. We propose an alternative strategy that allows direct manipulation of joint positions using local attraction or repulsion forces defined on a small set of local control points. Deformation fields generated from such point sources are determined by the choice of a Radial Basis Function (RBF). The Gaussian RBFs used in Figure 4 allow decoupling interaction strength s and interaction extent σ for each point on a joint located at a distance r as $\frac{s}{\sigma\sqrt{2\pi}} \exp\left(-\frac{r^2}{2\sigma}\right)$. A positive s indicates a radially repulsive point, while a negative value defines a radially attractive point. The strength and extent of the points actions can be adjusted dynamically, allowing for real-time user interaction. This addition enhances the versatility and applicability of the proposed approach, offering designers a comprehensive toolkit for exploring C-shell layouts.

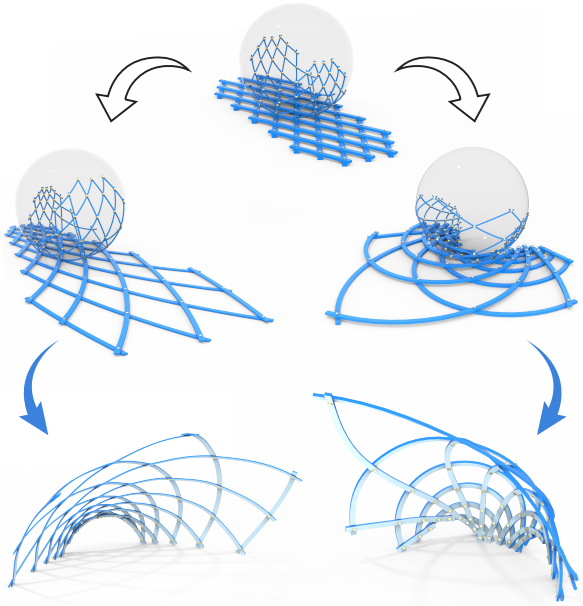


Figure 3: Variations of a reference linkage template (top left) using 2D Möbius transformations. The initial layout is projected onto the sphere, rotated about the sphere center, and projected back to the plane.

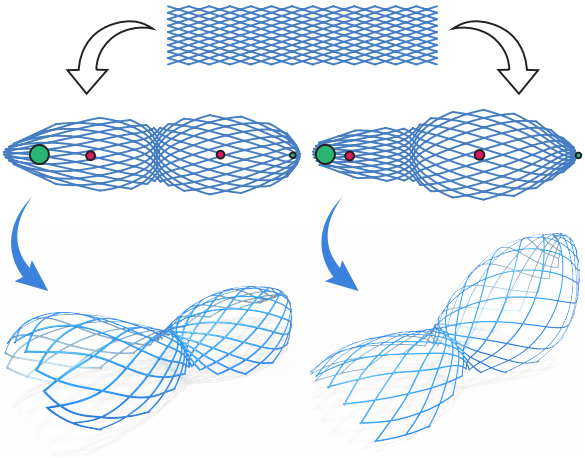


Figure 4: A reference linkage (top) is deformed using attractive and repulsive points laid out in the plane with varying action strengths. Green points attract neighboring joints with an intensity proportional to their radii, similar to red points repulsing neighboring joints. Gaussian RBFs with a single shared extent and varying strengths are chosen in these designs.

6. Linkage Topology Design

In the preceding section, we introduced techniques for manipulating joint angles and distances, offering means to adjust the geometry of the planar linkage layouts. Expanding on these methods, we now turn our attention to the topology of linkage grids. Navigating the full space of linkage topologies is difficult due to the combinatorial explosion of possibilities. We therefore expose a subset of such linkage topologies and facilitate direct user edits supported by automatic deletion of joints based on geometric criteria and tolerances.

6.1. Topology Families

Rectangular Lattice Topology. One straightforward approach is to use either rectangular or rhombic unit cells and tile them following a rectangular lattice in a 2D Euclidean space, see Figure 6. The number of joints and the spacing in the x and y directions can be tuned independently before applying our in-plane deformations tools discussed above.

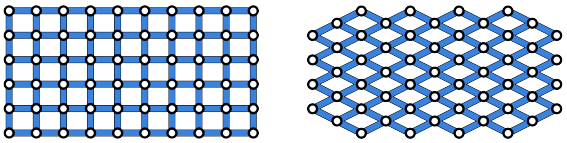


Figure 6: Rectangular lattices with rectangular (left) and rhombic (right) unit cells.

Annulus Topology. In addition to this, we allow users to design radially symmetric designs by adapting the rectangular lattice topology to polar coordinates. Joints in the 2D space are parameterized using polar coordinates i.e., they belong to $\mathcal{S}^1 \times \mathbb{R}_+$ where $\mathcal{S}^1$ is the unit circle.

An annulus topology is initialized from a rectangular lattice topology, for which the rectangle is axis-aligned in $\mathcal{S}^1 \times \mathbb{R}_+$, with a side length of 2π along the azimuthal direction to ensure periodicity, see Figure 5 on the left. Overlapping joints on the rectangle sides are identified so that all curves share

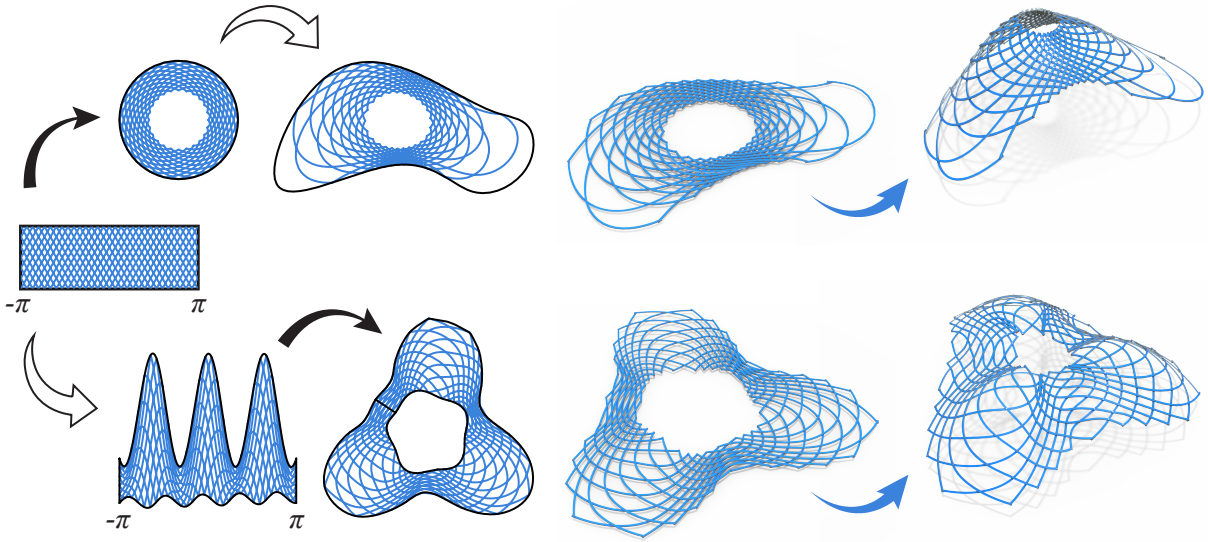


Figure 5: Our boundary-based deformations are compatible with other linkage representation spaces, allowing for finer control on annulus topologies. Converting a rectangular lattice linkage topology made of rhombus cells in the polar coordinates domain (left) to the Euclidean space produces a linkage with an annulus topology (top row, left). Boundary First Flattening [21] only allows simply connected domains to be manipulated and discards the inner boundary. The designer can edit the outer ring exclusively. Instead, we let the user edit the rectangular boundary in the polar coordinates domain before pushing the design to the Euclidean space (bottom row). This allows the inner and outer rings to be manipulated independently.

the same number of joints. Joint positions can be recovered in the 2D plane by evaluating the polar coordinates.

Such linkages can be edited by manipulating the domain boundary in the 2D plane or directly on the cylinder $\mathcal{S}^1 \times \mathbb{R}_+$. For the latter, we allow the designer to manipulate the sides of the rectangle along the radial direction and impose both sides to match along the azimuthal direction. This last property ensures that the deformation is well-defined on the unit circle.

While this second option affects the deployability of the linkage i.e., its opening angle distribution, it allows for a finer control of the inner circle of topology by decoupling it from the outer ring, see Figure 5.

6.2. Topology Editing

As the initial linkage deforms in the design process, some rod segments may grow unrealistically long. We detect such outliers and let the user discard them based on an adjustable length threshold. The remaining single valence joints are discarded iteratively until none can be found in the linkage. Alternatively, we let users manually remove joints and subsequently filter out single valence joints.

7. Implementation

Our C-shell design tools are packaged in a single Rhino-Grasshopper [23] plugin, see Figure 7. We split them into categories: Geometric Edits, Deployment, and Design Evaluation.

Geometric Edits encompass the abovementioned techniques, including boundary-induced deformations, Möbius transforms, attractive and repulsive points, and polar coordinates representation. The resulting linkage is simulated in the flat state and deployed according to Equation (1). The user controls the

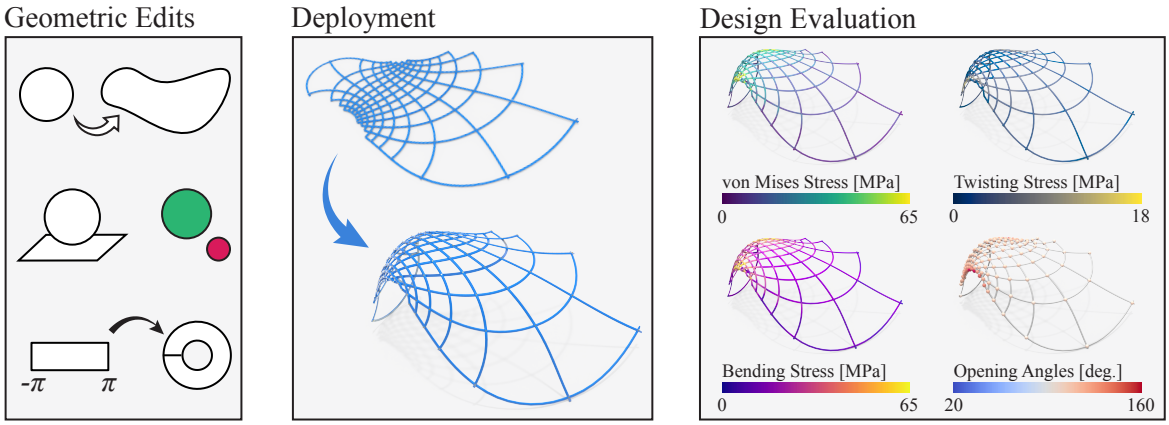


Figure 7: Overview of the functionalities available in our Rhino-Grasshopper [23] plugin.

deployment extent, and pinned joints if any. Physics quantities can be measured and are made available to the user following the model presented in Becker et al. [15]. As an example, Figure 7 shows the maximum von Mises stress at each vertex of the linkage discretization, where the scale is cropped at the yield stress of Acetal Copolymer (POM-C).

8. Conclusion

The incorporation of planar curved beams in C-shells represents a promising alternative for the design of elastic gridshells. The research presented in this paper aims to advance the forward design process of C-shells by introducing a comprehensive framework of human-interpretable manipulations of a reference linkage, inspired by considerations of scissor linkage deployability.

Our approach enables designers to navigate the intricate landscape of C-shell design with greater ease. By offering a set of intuitive strategies based on both conformal and non-conformal deformations within various topology layouts, we facilitate real-time recombination and modification of planar linkages. Through visual feedback of the resulting deployed state, designers can intuitively assess the impact of their design decisions and iteratively refine their creations.

While our research has demonstrated the vast design space that C-shells could offer, efforts are still required to address their scalability, particularly in terms of material efficiency and fabrication feasibility. However, by embracing the possibilities offered by C-shells, our research sets the stage for further innovation and exploration in the field of elastic gridshells.

Acknowledgments

This research was supported by the Swiss National Science Foundation (Grant FNS 188582 / CF 1156).

References

[1] B. Burkhardt and F. Otto, *Multihalle Mannheim; the documentation on the design and execution work of Mannheim Hall* (IL (Collection)). Krämer, 1978, ISBN: 9783782820134.

[2] C. Douthe, R. Mesnil, H. Orts, and O. Baverel, "Isoradial meshes: Covering elastic gridshells with planar facets," *Automation in Construction*, vol. 83, pp. 222–236, 2017, ISSN: 0926-5805. DOI: 10.1016/j.autcon.2017.08.015.

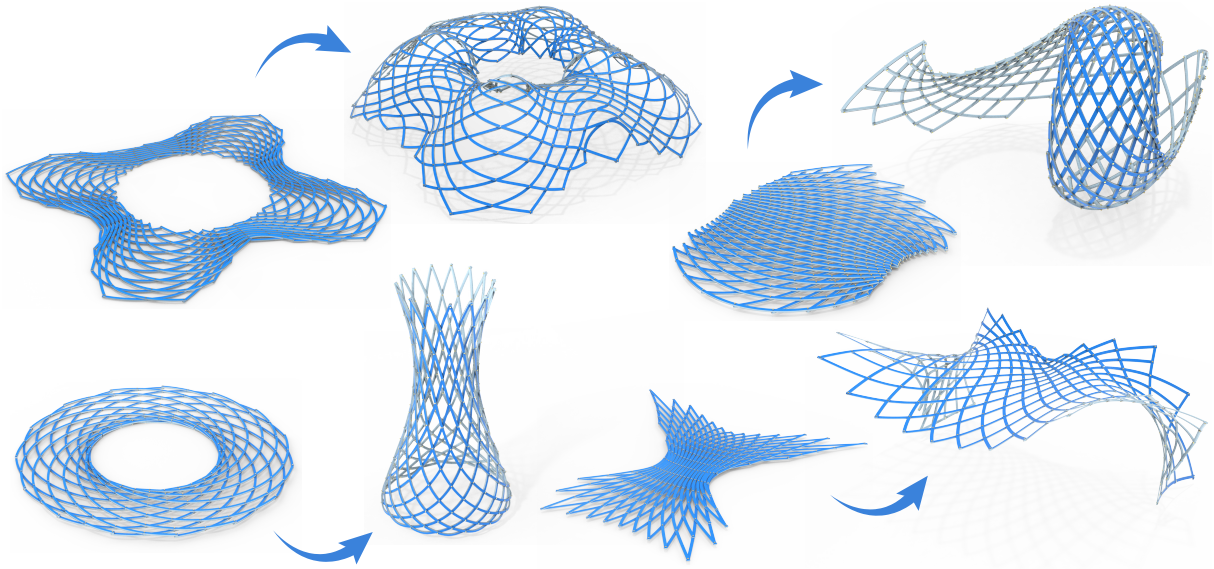


Figure 8: Compositions of edits produce designs with diverse-looking deployed states.

[3] C. Baek, A. O. Sageman-Furnas, M. K. Jawed, and P. M. Reis, "Form finding in elastic gridshells," *Proceedings of the National Academy of Sciences*, vol. 115, no. 1, pp. 75–80, 2018. DOI: 10.1073/pnas.1713841115.

[4] A. Garg *et al.*, "Wire mesh design," *ACM Trans. Graph.*, vol. 33, no. 4, Jul. 2014, ISSN: 0730-0301. DOI: 10.1145/2601097.2601106.

[5] A. O. Sageman-Furnas, A. Chern, M. Ben-Chen, and A. Vaxman, "Chebyshev nets from commuting polyvector fields," *ACM Trans. Graph.*, vol. 38, no. 6, Nov. 2019, ISSN: 0730-0301. DOI: 10.1145/3355089.3356564.

[6] D. Liu, D. Pellis, Y.-C. Chiang, F. Rist, J. Wallner, and H. Pottmann, "Deployable strip structures," *ACM Trans. Graph.*, vol. 42, no. 4, Jul. 2023, ISSN: 0730-0301. DOI: 10.1145/3592393.

[7] J. Panetta, M. Konaković-Luković, F. Isvoranu, E. Bouleau, and M. Pauly, "X-shells: A new class of deployable beam structures," *ACM Transactions on Graphics (TOG)*, vol. 38, no. 4, pp. 1–15, 2019. DOI: 10.1145/3306346.3323040.

[8] S. Pillwein, K. Leimer, M. Birsak, and P. Musialski, "On elastic geodesic grids and their planar to spatial deployment," *ACM Transactions on Graphics (TOG)*, vol. 39, no. 4, pp. 125–1, 2020. DOI: 10.1145/3386569.3392490.

[9] S. Pillwein and P. Musialski, "Generalized deployable elastic geodesic grids," *ACM Trans. Graph.*, vol. 40, no. 6, Dec. 2021, ISSN: 0730-0301. DOI: 10.1145/3478513.3480516.

[10] E. Soriano, R. Sastre, and D. Boixader, "G-shells:flat collapsible geodesic mechanisms for gridshells," in *International Conference Form and Force / Symposium of the International Association for Shell and Spatial structures / International Conference on Textile Composites and Inflatable Structures*, International Centre for Numerical Methods in Engineering (CIMNE), Oct. 2019, p. 1894.

[11] E. Schling, M. Kilian, W. Hui, J. Schikore, and H. Pottmann, "Design and construction of curved support structures with repetitive parameters," in *Advances in Architectural Geometry (AAG)*, Sep. 2018, ISBN: 978-3-903015-13-5.

[12] Y. Ren *et al.*, "3d weaving with curved ribbons," *ACM Transactions on Graphics (TOG)*, vol. 40, no. 4, pp. 1–15, 2021. DOI: 10.1145/3450626.3459788.

[13] C. Baek, A. G. Martin, S. Poincloux, T. Chen, and P. M. Reis, "Smooth triaxial weaving with naturally curved ribbons," *Phys. Rev. Lett.*, vol. 127, p. 104 301, 10 Aug. 2021. DOI: 10.1103/PhysRevLett.127.104301.

[14] S. Mhatre *et al.*, "Deployable structures based on buckling of curved beams upon a rotational input (adv. funct. mater. 35/2021)," *Advanced Functional Materials*, vol. 31, no. 35, p. 2 170 261, 2021. DOI: https://doi.org/10.1002/adfm.202170261.

[15] Q. Becker, S. Suzuki, Y. Ren, D. Pellis, J. Panetta, and M. Pauly, "C-shells: Deployable gridshells with curved beams," *ACM Trans. Graph.*, vol. 42, no. 6, Dec. 2023, ISSN: 0730-0301. DOI: 10.1145/3618366.

[16] G. Farin, *Curves and surfaces for CAGD: a practical guide*, 5th. San Francisco, CA, USA: Morgan Kaufmann Publishers Inc., 2001, ISBN: 1558607374.

[17] M. Bergou, M. Wardetzky, S. Robinson, B. Audoly, and E. Grinspun, "Discrete elastic rods," in *ACM SIGGRAPH 2008 papers*, 2008, pp. 1–12. DOI: 10.1145/1399504.1360662.

[18] M. Bergou, B. Audoly, E. Vouga, M. Wardetzky, and E. Grinspun, "Discrete viscous threads," *ACM Transactions on graphics (TOG)*, vol. 29, no. 4, pp. 1–10, 2010. DOI: 10.1145/1778765.1778853.

[19] J. C. Klann, "Walking device," US Patent 6,364,040, Apr. 2002.

[20] M. Eck, T. DeRose, T. Duchamp, H. Hoppe, M. Lounsbery, and W. Stuetzle, "Multiresolution analysis of arbitrary meshes," in *Proceedings of the 22nd annual conference on Computer graphics and interactive techniques*, 1995, pp. 173–182.

[21] R. Sawhney and K. Crane, "Boundary first flattening," *ACM Transactions on Graphics (ToG)*, vol. 37, no. 1, pp. 1–14, 2017. DOI: 10.1145/3132705.

[22] J. L. Walsh, "History of the riemann mapping theorem," *The American Mathematical Monthly*, vol. 80, no. 3, pp. 270–276, 1973.

[23] R. McNeel *et al.*, *Rhinoceros 3d (version 8.0)*, 2009.